Far-field properties of a cylindrically polarized vector beam and its beam quality beyond the paraxial approximation

Xinting Jia (贾信庭), Bo Li (李 波), and Youqing Wang (王又青)*

College of Optoelectronic Science and Engineering, Huazhong University of Science and Technology, Wuhan 430074, China

**E-mail: yqwang13@163.com*

Received September 3, 2009

The far-field analytical expressions for the electromagnetic fields of a cylindrically polarized vector beam propagating in free space are obtained based on the vector angular spectrum and the method of stationary phase. The far-field energy flux distributions and the beam quality by the power in the bucket (PIB) in the nonparaxial regime have been investigated. The PIB of the cylindrically polarized beam depends on the ratio of the waist width to wavelength, the order of the Laguerre polynomial, and the angle between the electrical vector and the radial direction. The analyses show that azimuthal polarization compared with radial polarization has better energy focusability in the far field.

OCIS codes: 260.2110, 350.5500, 260.5430.

doi: 10.3788/COL20100805.0517.

Different from the conventional polarizations, a new class of nonuniformly polarized beams, namely, the spirally polarized beams, was introduced by Gori[1]. As a particular case of the nonuniform polarizations, a cylindrically polarized beam has drawn a growing interest in some applications due to the cylindrical symmetry of its electrical vector, for example, electron acceleration, particle trapping, and material processing[2−4]. To the best of our knowledge, the focusing properties and applications of the cylindrically polarized beams have been extensively studied[5,6], but their beam quality beyond the paraxial approximation is less considered. In some practical applications the power in the bucket (PIB) is a useful beam quality characteristic parameter for measuring the power (energy) focusability of laser beams in the far field. In this letter, the properties of a cylindrically polarized vector beam in the far field and its beam quality based on PIB in the nonparaxial regime are investigated.

The transverse electric field distribution of a cylindrically polarized Laguerre-Gaussian beam (LGB) at the plane $z = 0$ reads as[7]

$$\mathbf{E}_{\perp}(x, y, 0) = E_{n1x}(x, y, 0)\mathbf{e}_x + E_{n1y}(x, y, 0)\mathbf{e}_y, \quad (1)$$

$$E_{n1x}(x, y, 0) = \cos(\phi + \varphi)\sqrt{2}E_0 \frac{\rho}{\omega_0} L_n^1\left(\frac{2\rho^2}{\omega_0^2}\right) \exp\left(-\frac{\rho^2}{\omega_0^2}\right), \quad (2)$$

$$E_{n1y}(x, y, 0) = \sin(\phi + \varphi)\sqrt{2}E_0 \frac{\rho}{\omega_0} L_n^1\left(\frac{2\rho^2}{\omega_0^2}\right) \exp\left(-\frac{\rho^2}{\omega_0^2}\right), \quad (3)$$

where $\mathbf{e}_x$ and $\mathbf{e}_y$ are the unit vectors in the x and y directions, respectively, $\rho = \sqrt{x^2 + y^2}$ and $\varphi = \arctan(y/x)$ are the polar coordinates, ϕ is a constant angle between the electrical vector and the radial direction, E_0 is an amplitude constant, ω_0 is the waist width of the fundamental mode, and $L_n^1(\cdot)$ is the Laguerre polynomial of order n and index 1. The geometry of the transverse electric field of a cylindrically polarized vector beam is shown in Fig. 1. One can note that each point of the beam cross section is a linear polarization rotated by ϕ from the radial direction. When $\phi = 0$, cylindrical polarization degenerates into radial polarization, whereas, for $\phi = \pi/2$, it reduces to azimuthal polarization.

By using the vector angular spectrum method[8], the propagating electric field of a cylindrically polarized LGB is obtained:

$$\mathbf{E}_{n1}(\mathbf{r}) = \int\int_{-\infty}^{+\infty} \left\{ A_{n1x}(p, q)\mathbf{e}_x + A_{n1y}(p, q)\mathbf{e}_y - \frac{\mathbf{e}_z}{m}\left[pA_{n1x}(p, q) + qA_{n1y}(p, q)\right] \right\} \cdot \exp\left[\mathrm{i}k(px + qy + mz)\right] \mathrm{d}p\mathrm{d}q, \quad (4)$$

where $\mathbf{r} = x\mathbf{e}_x + y\mathbf{e}_y + z\mathbf{e}_z$, $\mathbf{e}_z$ is the unit vector in the z direction, k is the wave number, and $m = \sqrt{1 - p^2 - q^2}$. $A_{n1x}(p, q)$ and $A_{n1y}(p, q)$ are the Fourier transform of the initial electric field $E_{n1x}(x, y, 0)$ and $E_{n1y}(x, y, 0)$, respectively.

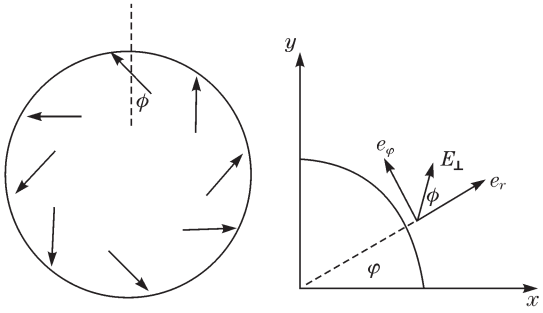

Fig. 1. Cylindrically polarized beam with an angle ϕ between the electrical vector and the radial direction.

$$A_{n1x}(p,q) = \frac{1}{\lambda^2}\int\int_{-\infty}^{+\infty} E_{n1x}(x,y,0)\exp\left[-\mathrm{i}k(px+qy)\right]\mathrm{d}x\mathrm{d}y$$
$$= \mathrm{i}(-1)^{n+1}\sqrt{2}E_0(p\cos\phi - q\sin\phi)\frac{\pi^2\omega_0^3}{\lambda^3}L_n^1\left[\frac{(kb\omega_0)^2}{2}\right]\exp\left[-\left(\frac{kb\omega_0}{2}\right)^2\right], \quad (5)$$

$$A_{n1y}(p,q) = \frac{1}{\lambda^2}\int\int_{-\infty}^{+\infty} E_{n1y}(x,y,0)\exp\left[-\mathrm{i}k(px+qy)\right]\mathrm{d}x\mathrm{d}y$$
$$= \mathrm{i}(-1)^{n+1}\sqrt{2}E_0(q\cos\phi + p\sin\phi)\frac{\pi^2\omega_0^3}{\lambda^3}L_n^1\left[\frac{(kb\omega_0)^2}{2}\right]\exp\left[-\left(\frac{kb\omega_0}{2}\right)^2\right], \quad (6)$$

where $b=\sqrt{p^2+q^2}$ and λ is the wavelength. By taking the curl of Eq. (4), the propagating magnetic field of a cylindrically polarized LGB is given:

$$\mathbf{H}_{n1}(\mathbf{r}) = \sqrt{\frac{\varepsilon}{\mu}}\int\int_{-\infty}^{+\infty}\left\{\begin{array}{l} -\left[\frac{pq}{m}A_{n1x}(p,q)+\frac{1-p^2}{m}A_{n1y}(p,q)\right]\mathbf{e}_x \\ +\left[\frac{1-q^2}{m}A_{n1x}(p,q)+\frac{pq}{m}A_{n1y}(p,q)\right]\mathbf{e}_y \\ -\left[qA_{n1x}(p,q)-pA_{n1y}(p,q)\right]\mathbf{e}_z \end{array}\right\}\exp\left[\mathrm{i}k(px+qy+mz)\right]\mathrm{d}p\mathrm{d}q, \quad (7)$$

where ε is the electric permittivity and μ is the magnetic permeability.

According to the method of stationary phase[9−11], the corresponding analytical expressions of the electromagnetic fields in the far field can be derived under the condition of $kr\to\infty$ and $r=\sqrt{x^2+y^2+z^2}$, that is,

$$\mathbf{E}_{n1}(\mathbf{r}) = \left[(x\cos\phi - y\sin\phi)z\mathbf{e}_x + (y\cos\phi + x\sin\phi)z\mathbf{e}_y - \rho^2\cos\phi\mathbf{e}_z\right]$$
$$\times\ (-1)^{n+1}\sqrt{2}E_0\frac{\pi^2\omega_0^3}{\lambda^2 r^3}L_n^1\left[\frac{(k\rho\omega_0)^2}{2r^2}\right]\exp\left[\mathrm{i}kr-\left(\frac{k\rho\omega_0}{2r}\right)^2\right], \quad (8)$$

$$\mathbf{H}_{n1}(\mathbf{r}) = \sqrt{\frac{\varepsilon}{\mu}}\left[\left(\frac{y}{z}\cos\phi+\frac{xz}{r^2}\sin\phi\right)\mathbf{e}_x - \left(\frac{x}{z}\cos\phi-\frac{yz}{r^2}\sin\phi\right)\mathbf{e}_y - \frac{\rho^2}{r^2}\sin\phi\mathbf{e}_z\right]$$
$$\times\ (-1)^{n}\sqrt{2}E_0\frac{\pi^2\omega_0^3 z}{\lambda^2 r^2}L_n^1\left[\frac{(k\rho\omega_0)^2}{2r^2}\right]\exp\left[\mathrm{i}kr-\left(\frac{k\rho\omega_0}{2r}\right)^2\right]. \quad (9)$$

The energy flux distribution at the plane $z=$ constant in the far field is described by the z component of the time-average Poynting vector $\langle S_z\rangle = \frac{1}{2}\mathrm{Re}[\mathbf{E_{n1}}(\mathbf{r})\times\mathbf{H}^*_{\mathbf{n1}}(\mathbf{r})]_z$, where Re is the real part and $*$ denotes the complex conjugate. As an alternative approach for characterizing the beam quality in the far field[12,13], the PIB in the nonparaxial regime is presented:

$$\mathrm{PIB} = \frac{\int_{-b_x}^{b_x}\int_{-b_y}^{b_y}\langle S_z\rangle\,\mathrm{d}x\mathrm{d}y}{\int\int_{-\infty}^{+\infty}\langle S_z\rangle\,\mathrm{d}x\mathrm{d}y}, \quad (10)$$

where b_x and b_y are the bucket half-widths in the x and y directions, respectively. The larger value of PIB means the better beam quality and the better energy focusability in the far field.

Figure 2 exhibits the energy flux distributions of a cylindrically polarized LGB at the plane $z=100\lambda$ and $\phi=0$ in the cases of (a) $n=0$, $\omega_0/\lambda=0.5$, (b) $n=0$, $\omega_0/\lambda=1$, (c) $n=1$, $\omega_0/\lambda=1$, and (d) $n=2$, $\omega_0/\lambda=1$. Note that the energy flux retains cylindrical symmetry and has dark center, and its profile expands with n increasing and ω_0/λ decreasing. The number of the outer rings depends on the order n.

The PIB curves of a cylindrically polarized LGB versus $b_x=b_y=b/\lambda$ at the plane $z=100\lambda$ are presented in Fig. 3(a) for different values of $\omega_0/\lambda=1$, 0.75, 0.5, $n=0$, $\phi=0$, in Fig. 3(b) for different values of $n=0$, 1, 2, $\omega_0/\lambda=1$, $\phi=0$, and in Fig. 3(c) for different values of $\phi=\pi/2$, $\pi/4$, 0, $\omega_0/\lambda=0.75$, $n=1$. Figures. 3(a) and (b) indicate that the better energy focusability in the far field can be obtained with the larger ω_0/λ and the lower order n, which are explained in Fig. 2. From Fig. 3(c), one can note that the PIB depends on the

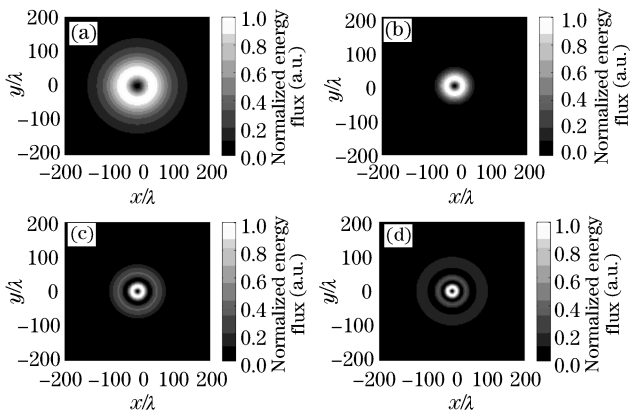

Fig. 2. Energy flux distribution of a cylindrically polarized LGB at the plane $z=100\lambda$ in the cases of (a) $n=0$, $\omega_0/\lambda=0.5$, (b) $n=0$, $\omega_0/\lambda=1$, (c) $n=1$, $\omega_0/\lambda=1$, and (d) $n=2$, $\omega_0/\lambda=1$, the parameter $\phi=0$.

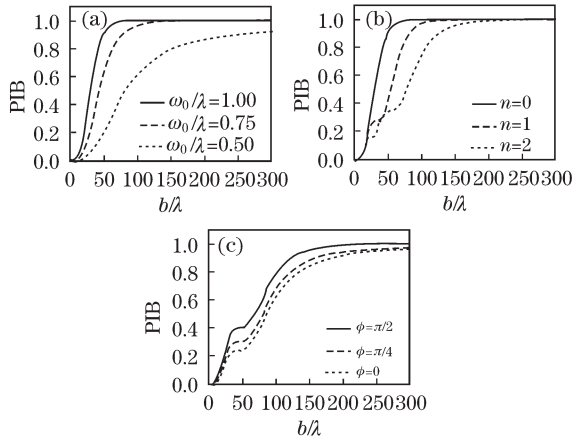

Fig. 3. PIB curves of a cylindrically polarized LGB at the plane $z = 100\lambda$ in the cases of (a) $\omega_0/\lambda = 1$, 0.75, 0.5, $n = 0$, $\phi = 0$, (b) $n = 0$, 1, 2, $\omega_0/\lambda = 1$, $\phi = 0$, and (c) $\phi = \pi/2$, $\pi/4$, 0, $\omega_0/\lambda = 0.75$, $n = 1$.

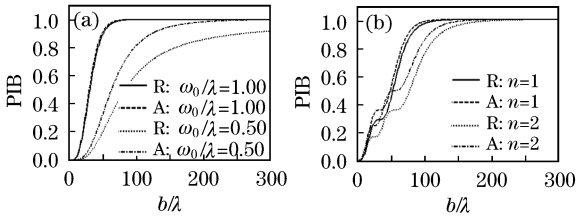

Fig. 4. PIB curves of radially ($\phi = 0$) and azimuthally ($\phi = \pi/2$) polarized LGBs at the plane $z = 100\lambda$ in the cases of (a) $\omega_0/\lambda = 1$, 0.5, $n = 0$ and (b) $n = 1$, 2, $\omega_0/\lambda = 1$. R and A denote the radial and azimuthal polarizations, respectively.

angle ϕ, and the PIB increases with the increasing ϕ in the region of $0 \leq \phi \leq \pi/2$. The PIB curves of radially ($\phi = 0$) and azimuthally ($\phi = \pi/2$) polarized LGBs versus b/λ at the plane $z = 100\lambda$ are plotted together for comparison in the cases of (a) $\omega_0/\lambda = 1$, 0.5, $n = 0$ and (b) $n = 1$, 2, $\omega_0/\lambda = 1$. From Fig. 4, one can find that azimuthal polarization compared with radial polarization has better beam quality and better energy focusability in the far field. The differences of the energy focusability between the radial and azimuthal polarizations are growing as ω_0/λ decreases and n increases. It implies that the profile of the energy flux $\langle S_z \rangle$ in the far field for azimuthal polarization is narrower than that for radial polarization.

In conclusion, the far-field analytical expressions for the electromagnetic fields of a cylindrically polarized LGB propagating in free space are presented. The far-field energy flux distributions and the beam quality on the basis of PIB beyond the paraxial approximation have been demonstrated. The numerical results show that azimuthal polarization compared with radial polarization has better energy focusability in the far field.

This work was supported by the National Key Technology Research and Development Program under Grant No. 2007BAF11B01.

References

1. F. Gori, J. Opt. Soc. Am. A **18,** 1612 (2001).
2. Y. I. Salamin and C. H. Keitel, Phys. Rev. Lett. **88,** 095005 (2002).
3. Q. Zhan, Opt. Express **12,** 3377 (2004).
4. M. Meier, V. Romano, and T. Feurer, Appl. Phys. A **86,** 329 (2007).
5. Q. Zhan and J. R. Leger, Opt. Express **10,** 324 (2002).
6. Z. Zhang, J. Pu, and X. Wang, Chinese J. Laser (in Chinese) **35,** 401 (2008).
7. A. A. Tovar, J. Opt. Soc. Am. A **15,** 2705 (1998).
8. C. G. Chen, P. T. Konkola, J. Ferrera, P. K. Heilmann, and M. L. Schattenburg, J. Opt. Soc. Am. A **19,** 404 (2002).
9. G. Zhou, Opt. Lett. **31,** 2616 (2006).
10. W. H. Carter, J. Opt. Soc. Am. **62,** 1195 (1972).
11. G. Zhou, X. Chu, and J. Zheng, Chin. Opt. Lett. **6,** 395 (2008).
12. A. E. Siegman, OSA TOPS **17,** 184 (1998).
13. X. Kang and B. Lü, Opt. Commun. **262,** 1 (2006).